NASA TECHNICAL NOTE

NASA TN D-2886

EFFECT OF BODY CROSS SECTION AND WIDTH-HEIGHT RATIO ON PERFORMANCE OF BODIES AND DELTA-WING—BODY COMBINATIONS AT MACH 6.9

by Allen H. Whitehead, Jr.

Langley Research Center
Langley Station, Hampton, Va.

NATIONAL AERONAUTICS AND SPACE ADMINISTRATION • WASHINGTON, D. C. • JUNE 1966

NASA TN D-2886

EFFECT OF BODY CROSS SECTION AND WIDTH-HEIGHT RATIO ON PERFORMANCE OF BODIES AND DELTA-WING—BODY COMBINATIONS AT MACH 6.9

By Allen H. Whitehead, Jr.

Langley Research Center
Langley Station, Hampton, Va.

NATIONAL AERONAUTICS AND SPACE ADMINISTRATION

For sale by the Clearinghouse for Federal Scientific and Technical Information
Springfield, Virginia 22151 – Price $1.00

EFFECT OF BODY CROSS SECTION AND WIDTH-HEIGHT RATIO ON PERFORMANCE OF BODIES AND DELTA-WING—BODY COMBINATIONS AT MACH 6.9

By Allen H. Whitehead, Jr.
Langley Research Center

SUMMARY

An investigation of the aerodynamic characteristics of bodies and wing-body combinations with triangular, rectangular, and elliptical body cross-sectional shapes and with body width-height ratios of 2 and 3 was conducted at a free-stream Mach number of 6.9 and a Reynolds number based on length of 1.4×10^6. The two delta wings tested in combination with these bodies had leading-edge sweep angles of 70^o and 75^o. All configurations were tested in both flat-top and flat-bottom orientations.

The results of the investigation show that for either bodies alone or wing-body combinations the possibility of an increase in the maximum lift-drag ratio $(L/D)_{max}$ with an increase in width-height ratio depends on the cross-sectional shape and the orientation (flat top or flat bottom) of the configuration. For the flat-top wing-body combinations, neither the small increase in width-height ratio nor the change in cross-sectional shape from the basic conical to a triangular, rectangular, or elliptical wing-body combination produces any significant increase in $(L/D)_{max}$. In contrast, for the flat-bottom wing-body combinations, body cross-sectional deviations from the conical body in some instances are shown to provide higher values of $(L/D)_{max}$.

INTRODUCTION

The present investigation was undertaken as a part of a systematic research program initiated at the Langley Research Center to provide aerodynamic principles for developing high lift-drag ratios for bodies and various wing-body combinations at hypersonic speeds. The scope of this general study and summaries of major results obtained to date are reported in references 1 and 2, and references 3 to 6 present detailed information on the various configurations tested. The investigations reported in references 4 and 5 were devoted to a study of favorable interference effects on half-cone delta-wing configurations (suggested by Eggers and Syvertson in ref. 7) at Mach numbers of 6.9 in air and 20 in helium. Results of an investigation of the effects on performance at Mach 6.8 produced by modifications to the wing planform and the addition of afterbodies are reported in reference 6.

The purpose of the present investigation was to study the effect of changing body cross-sectional shape and width-height ratio on the aerodynamic characteristics of these delta-wing configurations. In order to aid in the evaluation of the effects of these modifications, the bodies were designed so that with a given wing attached to any body, the volume parameter (volume$^{2/3}$ divided by planform area) was a constant value.

SYMBOLS

b	body width
b/h	body width-height ratio
C_A	axial-force coefficient, $\frac{\text{Axial force}}{q_\infty S}$
C_D	drag coefficient, $\frac{\text{Drag}}{q_\infty S}$
C_L	lift coefficient, $\frac{\text{Lift}}{q_\infty S}$
$C_{L,opt}$	optimum lift coefficient, C_L at $(L/D)_{max}$
C_m	pitching-moment coefficient, $\frac{\text{Pitching moment}}{q_\infty S\bar{c}}$
C_N	normal-force coefficient, $\frac{\text{Normal force}}{q_\infty S}$
$\bar{c}$	mean aerodynamic chord
c_r	root chord
d	diameter
h	body height
L/D	lift-drag ratio
$(L/D)_{max}$	maximum value of lift-drag ratio
p_b	base pressure
p_∞	free-stream pressure

q_∞ free-stream dynamic pressure

R Reynolds number based on model length

S planform area

s wing semispan

V configuration volume (including wing volume on wing-body combination)

x distance from aerodynamic center to moment reference point (positive forward)

α angle of attack

Θ semiapex angle of body in vertical plane

Λ leading-edge sweep angle

ξ semiapex angle of body in horizontal plane

φ wedge angle of wings normal to leading edge

Abbreviations:

FB flat-bottom configuration (body mounted above wing)

FT flat-top configuration (body mounted below wing)

CONFIGURATIONS

The dimensions of the bodies and wings used in the investigation are shown in figure 1. Bodies with rectangular, triangular, and elliptical cross sections having width-height ratios of 2 and 3 are investigated with and without wings attached. The elliptical body with a width-height ratio of 2 is a half cone. The two wings have leading-edge sweep angles of 70° and 75° and are equal in length to the bodies. The bodies were designed to have a constant volume so that the volume parameter ($V^{2/3}/S$) for all wing-body combinations involving the 70° swept wing is 0.127 and the volume parameter for all wing-body combinations involving the 75° swept wing is 0.177. The wing leading-edge

thickness is maintained at 0.0254 cm. All models are tested in both flat-top and flat-bottom orientations.

APPARATUS, TESTS, AND ACCURACY

The investigation was conducted in the Langley 11-inch hypersonic tunnel described in reference 8. The facility is of the blowdown type with test durations of about a minute. A nominal Mach number of 6.9 in air is produced by a contoured two-dimensional nozzle constructed from invar so that contraction and expansion of the throat due to heat absorption is minimized. The Mach number variation during the test run is only about 1 percent after the first 10 seconds. A calibration of this nozzle can be found in reference 9.

The tests were conducted at a Mach number of 6.86 at a stagnation temperature of 617° K and a stagnation pressure of 16 atmospheres (1.6 MN/m^2). The corresponding Reynolds number based on model length was 1.4×10^6. The water vapor content in the air was maintained sufficiently low to eliminate water condensation effects.

Forces and moments on the models were measured by an external three-component strain-gage balance that was water-cooled to minimize the effects of heating. Base-pressure measurements were required to adjust the axial-force data to a free-stream condition in which there is no base-pressure contribution to the aerodynamic loading. The pressure recorder was a six-cell mechanical-optical unit described in detail in reference 8. This unit converts the deflection of a diaphragm into a rotation of a small mirror which in turn reflects a beam of light onto a moving film. Because of the slow response of these mechanical-optical units, separate tests were made in which selected models were tested at a constant angle of attack to insure accurate base-pressure determination. The base-pressure values were found to be insensitive to changes in body cross section or width-height ratio; therefore, a curve of base pressure plotted as a function of angle of attack was constructed to provide a single base-pressure value for all configurations at a given angle of attack. After the tests had been performed, a high-response transducer became available for obtaining base-pressure data. Figure 2 presents the base-pressure values for two configurations obtained by the transducer as well as the standard base-pressure curve that was used in the reduction of the data. Included in the figure is the range of error due to any inaccuracy of the mechanical-optical recorder; it can be seen that the maximum error in assuming base pressure independent of base shape was no greater than the error due to inaccuracy of the original pressure instrumentation. The contribution of base-pressure error to error in $(L/D)_{max}$ is estimated to be ± 0.08. The balance sting and shield and base-pressure-tube arrangement are also shown in figure 2.

The angle of attack of the models was referenced to the flat surface of the wings for the wing-body combinations and to the flat portion of the body for the body-alone configurations. The model angle of attack was set by means of the reflection of a monochromatic light beam from a small prism embedded in the model surface on a precalibrated board outside the tunnel. The angle of attack could thus be determined without concern for sting and model deflection due to aerodynamic loading. The angle of attack determined by this method is accurate within $\pm 0.2^{\circ}$.

The cumulative errors in the aerodynamic coefficients due to the aforementioned uncertainties and to errors in measuring the forces and moments are estimated as follows:

	Bodies alone	Wing-body combinations
C_L	±0.003	±0.001
C_D	±0.0015	±0.0006
L/D	±0.32	±0.20
C_m	±0.003	±0.001

However, repeatability of the test data indicates that the errors in the force coefficients were never this great.

RESULTS AND DISCUSSION

Basic Data

The basic data are presented in figure 3. The model attitudes are identical in the flat-top and flat-bottom orientations when the flat-top configurations are at $\alpha = -2^{\circ}$ and the flat-bottom configurations are at $\alpha = 2^{\circ}$; the attitudes are also the same for the two orientations at $\alpha = 0^{\circ}$. A common fairing was therefore used which is influenced by the data of both model orientations. For this reason the curve does not necessarily pass through the symbols at low angles of attack. Figures 3(a) and 3(b) present the data for the bodies alone, and these results show that the rectangular body has the largest axial-force coefficient in either flat-top or flat-bottom orientation. These larger values of C_A for the rectangular body are partly due to the fact that the coefficients are referenced to the planform area which is smaller for the rectangular body than for the other bodies with the same width-height ratio.

The shaded symbols in figure 3(a) denote the theoretical prediction of the inviscid axial-force coefficient at zero incidence and the shaded symbols with flags denote the theoretical prediction of the total axial-force coefficient at zero incidence. The inviscid

values were obtained from oblique shock theory, and the estimates of the contribution of laminar skin friction to the total drag were made by a method which includes the effects of boundary-layer displacement. The difference in magnitude of the values represented by the unflagged symbols and those indicated by the flagged symbols at $\alpha = 0^{o}$ is the value of the skin-friction contribution. It can be seen that at $\alpha = 0^{o}$ the skin friction is nearly independent of body shape. Thus, the value of C_A at $\alpha = 0^{o}$ for the rectangular body is higher than that for the other bodies because of the higher inviscid drag.

In general, the flat-top rectangular body alone has higher normal-force coefficients than the other bodies (fig. 3(a)); however, because of the higher values of C_A, the values of L/D fall below those for the elliptical and triangular bodies without wings. The lift-drag characteristics of the flat-top elliptical and triangular bodies show only slight dissimilarities, the triangular configuration producing slightly greater values of L/D throughout the angle-of-attack range. The lower value of $(L/D)_{max}$ of the rectangular body alone in the flat-bottom orientation (fig. 3(b)) is again traced to a higher value of C_A at $(L/D)_{max}$. The triangular body alone in this orientation has the highest value of $(L/D)_{max}$ of the three bodies because it has the lowest value of C_A.

Figures 3(c) to 3(f) present the basic data for the wing-body combinations. The values of C_N are nearly independent of the cross section of the body with either wing attached. The values of C_A, however, do show a variation with change in body cross section. As in the body-alone data, the rectangular wing-body combination produces the highest values of C_A, again causing a loss in the lift-drag ratio throughout the angle-of-attack range. In the flat-top configurations (figs. 3(c) and 3(e)), the elliptical combinations generally show higher values of $(L/D)_{max}$, whereas in the reversed orientation (figs. 3(d) and 3(f)), the triangular wing-body combinations show superior performance.

Maximum Lift-Drag-Ratio Characteristics

In figure 4(a), the maximum lift-drag-ratio characteristics for the bodies alone are shown. As was shown in figure 3 for either value of b/h the rectangular body suffers a penalty in efficiency for both flat-top and flat-bottom orientations. In either orientation, the triangular body alone provides the highest value of $(L/D)_{max}$.

With the 75^{o} and 70^{o} swept wings attached to the bodies, the values of $(L/D)_{max}$ are greater than those for the bodies alone for all configurations (figs. 4(b) and 4(c)). The efficiencies of the wing-body combinations remain in the same relation as that described previously for the body alone; that is, the rectangular body with either wing attached still shows the poorest performance when compared with that of the other wing-body combinations. The reasons for these lower values of $(L/D)_{max}$ for the rectangular body were discussed in the Basic Data section. The values of $(L/D)_{max}$ for the wing-body combinations in the flat-top orientation are influenced to only a small extent by the change in body

cross-sectional shape; the elliptical wing-body configurations generally show slightly greater values of $(L/D)_{max}$, but the greatest increase is less than 4 percent. In the reversed orientation, however, the choice of cross-sectional shape above the wing does influence the performance of the configurations. The triangular wing-body combinations are superior, providing up to an 8-percent increase in values of $(L/D)_{max}$ over the values for the winged configurations with the elliptical body.

A major difference in performance between the 70^{o} and 75^{o} swept wing combinations can be seen in the values of $(L/D)_{max}$ for the flat-top orientation as compared with the flat-bottom results. For all the 75^{o} swept wing-body combinations, the flat-top orientation produces a higher value of $(L/D)_{max}$ than its flat-bottom counterpart (fig. 4(b)). The reason for this behavior can be attributed to the interference effects generated by the body on the flow field over the wing. The criteria for which this interference phenomenon will provide the necessary favorable influence to generate greater values of $(L/D)_{max}$ for the flat-top configurations are discussed in detail in reference 4. If only the effect of Mach number normal to the leading edge on the shock detachment is considered, these criteria indicate that the value of $(L/D)_{max}$ for the flat-top configurations is greater only when the leading-edge shock of the flat-bottom wing-body combination detaches at an angle of attack below that for $(L/D)_{max}$. Leading-edge-diameter effects on shock detachment are not considered in detail in reference 4, but it was shown that these criteria are applicable to wings with small leading-edge bluntness as well as the idealized sharp-leading-edge wings. The leading-edge blunting present on the wings used in the investigation was small enough that the criteria are still applicable. Theoretically, the leading-edge shocks of the flat-bottom 75^{o} swept wing-body combinations are detached before the angles of attack for $(L/D)_{max}$ are reached; thus the criteria are satisfied and higher values of $(L/D)_{max}$ are obtained with the flat-top configurations. These interference benefits were not significantly affected by changes in body cross section or increases in the value of b/h. In contrast, there is no apparent difference in $(L/D)_{max}$ attributed to changing orientation of the configurations with the 70^{o} swept wing attached (fig. 4(c)). This result is consistent with the above results in that from a normal Mach number consideration, the leading-edge shocks of these flat-bottom configurations detach beyond the angles of attack for $(L/D)_{max}$.

Variation of Width-Height Ratio

The effect of the width-height ratio on the maximum lift-drag ratio can be seen in figure 5. It should be noted that the lines between the data points in figure 5 are presented to aid in comparing the configurations, and, as such, do not represent fairings which would allow interpolation of values of b/h between 2 and 3. Changing the value of b/h from 2 to 3 increases the value of $(L/D)_{max}$ for the triangular bodies alone and the flat-top elliptical body alone, but produces a negligible effect on the remainder of the bodies

without wings attached. Within the accuracy of the data, the effects of the width-height ratio on the efficiency parameter of the wing-body combinations are generally small, the exception to this result being provided by the flat-top elliptical body with the 75° swept wing attached (fig. 5(c)). The change in the ratio b/h from 2 to 3 for this wing-body combination results in an increase in $(L/D)_{max}$ of about 4 percent, which is still only a small improvement in performance. This insensitivity of $(L/D)_{max}$ to changes in the ratio b/h was corroborated for winged elliptic cones by results reported in reference 10 obtained at a Mach number of about 3. Whereas the width-height ratio (axis ratio in the terminology of ref. 10) was found in this reference to have a noticeable effect on the maximum lift-drag ratio for elliptic bodies alone, when a 70° swept wing was combined with these bodies, the changes in $(L/D)_{max}$ with variations in the ratio b/h were small. It was shown in figure 9(c) of reference 10 that at a Mach number of 2.94, changing the width-height ratio from 2 to 6 (this change corresponds to changing the axis ratio from 1 to 3 in ref. 10) increased the value of $(L/D)_{max}$ only 5 percent. Thus, the general result that was found for elliptical bodies in supersonic flow (ref. 10) is found to be valid at low hypersonic speeds (present tests): a small departure from a circular body cross section for a wing-body combination does not cause a significant change in the value of $(L/D)_{max}$.

All but one of the flat-top wing-body combinations produce increases in $(L/D)_{max}$ greater than 10 percent over the values for the flat-top body-alone configurations. (See fig. 5.) The exception is the triangular-cross-section body with a value of b/h of 3 in combination with the 75° swept wing. The reason for this result is that the planform area of this body nearly equals that of the wing above it, so that the increase in lift obtained by addition of the wing is small. Similarly, neither of the flat-bottom triangular wing-body configurations shows a large increase in $(L/D)_{max}$ over the results for the flat-bottom body alone, whereas the flat-bottom elliptical and rectangular wing-body combinations provide sizable increases in $(L/D)_{max}$ over the data for the body alone. The results in figure 5 also show that the magnitudes of $(L/D)_{max}$ for the 75° swept wing-body combinations are, in general, lower than those for the 70° swept wing-body combinations. However, the reduction in $(L/D)_{max}$ due to sweep is only about 5.5 percent or smaller for the flat-top configurations, a relatively minor penalty for a 26-percent decrease in wing area. A final observation to be made is that, in general, for the flat-top orientation the elliptical wing-body combinations show the highest values of $(L/D)_{max}$, whereas for the reversed orientation the triangular wing-body combinations show superior performance.

Figure 6 shows the effect of changing body cross section and width-height ratio on the parameter $C_{L,opt}$ (the lift coefficient at $(L/D)_{max}$). The data of figure 6 for the rectangular wing-body combinations show that within the error of the data there is no effect on $C_{L,opt}$ of the change in b/h. The elliptical wing-body configurations exhibit

a small increase in the values of this parameter with an increase in the value of b/h from 2 to 3, whereas the triangular wing-body combinations show a slight decrease in the values of $C_{L,opt}$. The flat-bottom wing-body combinations produce a larger value of $C_{L,opt}$ in all cases because the configurations in this orientation reach a maximum lift-drag ratio at a much larger angle of attack than their flat-top counterparts.

Aerodynamic Center

The aerodynamic-center location $x/\bar{c}$ was nearly constant for all configurations (fig. 7), varying from 1.2 to 2.6 percent of the mean aerodynamic chord ahead of the moment reference center. Thus, the aerodynamic reference center was located approximately 65 percent of the chord length from the apex. Figure 7 shows a slight variation of the reference center $x/\bar{c}$ with cross section, but there are no discernible trends.

CONCLUSIONS

An investigation of the aerodynamic characteristics of bodies and wing-body combinations with triangular, rectangular, and elliptical body cross-sectional shapes and with body width-height ratios of 2 and 3 was conducted at a free-stream Mach number of 6.9 and a Reynolds number based on length of 1.4×10^6. The two delta wings tested in combination with these bodies had leading-edge sweep angles of 70° and 75°. All configurations were tested in both flat-top and flat-bottom orientations. The results from this investigation led to the following conclusions:

1. For bodies alone, the maximum lift-drag ratio $(L/D)_{max}$ is affected by body cross-sectional shape. In the present tests the triangular cross section produced the highest values of $(L/D)_{max}$ at a given value of the width-height ratio. Improvement in $(L/D)_{max}$ through a small increase in the value of the width-height ratio is dependent on cross-sectional shape.

2. For the flat-top wing-body combinations, neither the small increase in width-height ratio nor the change in cross-sectional shape from the basic conical to a triangular, rectangular, or elliptical wing-body configuration produced any significant increase in $(L/D)_{max}$. For example, the maximum increase in $(L/D)_{max}$ was about 4 percent, which occurred when changing the value of b/h for the elliptical wing-body combination. In contrast, body cross-sectional shape effects can be important on the flat-bottom configurations since a maximum increase of about 8 percent in values of $(L/D)_{max}$ was obtained by changing the body cross section from elliptical to triangular.

3. Wing-body interference effects caused the flat-top configuration with the 75° leading-edge sweep wing to have higher values of $(L/D)_{max}$ than the comparable

flat-bottom configurations. In general, these interference benefits were not significantly affected by changes in body cross section or increases in the value of b/h.

4. The aerodynamic center of all configurations was found to be located about 65 percent of the chord length from the apex.

Langley Research Center,
National Aeronautics and Space Administration,
Langley Station, Hampton, Va., February 4, 1966.

REFERENCES

1. Fetterman, David E.; Henderson, Arthur, Jr.; Bertram, Mitchel H.; and Johnston, Patrick J.: Studies Relating to the Attainment of High Lift-Drag Ratios at Hypersonic Speeds. NASA TN D-2956, 1965.

2. Becker, John V.: Studies of High Lift/Drag Ratio Hypersonic Configurations. Proceedings of the 4th Congress of the International Council of the Aeronautical Sciences, Robert R. Dexter, ed., Spartan Books, Inc., 1965, pp. 877-910.

3. Penland, Jim A.: Maximum Lift-Drag-Ratio Characteristics of Rectangular and Delta Wings at Mach 6.9. NASA TN D-2925, 1965.

4. Fetterman, David E.: Favorable Interference Effects on Maximum Lift-Drag Ratios of Half-Cone Delta-Wing Configurations at Mach 6.86. NASA TN D-2942, 1965.

5. Johnston, Patrick J.; Snyder, Curtis D.; and Witcofski, Robert D.: Maximum Lift-Drag Ratios of Delta-Wing—Half-Cone Combinations at a Mach Number of 20 in Helium. NASA TN D-2762, 1965.

6. Small, William J.; and Bertram, Mitchel H.: Effect of Geometric Modifications on the Maximum Lift-Drag Ratios of Slender Wing-Body Configurations at Hypersonic Speeds. NASA TN D-3276, 1966.

7. Eggers, A. J., Jr.; and Syvertson, Clarence A.: Aircraft Configurations Developing High Lift-Drag Ratios at High Supersonic Speeds. NACA RM A55L05, 1956.

8. McLellan, Charles H.; Williams, Thomas W.; and Bertram, Mitchel H.: Investigation of a Two-Step Nozzle in the Langley 11-Inch Hypersonic Tunnel. NACA TN 2171, 1950.

9. Bertram, Mitchel H.: Exploratory Investigation of Boundary-Layer Transition on a Hollow Cylinder at a Mach Number of 6.9. NACA Rept. 1313, 1957. (Supersedes NACA TN 3546.)

10. Jorgensen, Leland H.: Elliptic Cones Alone and With Wings at Supersonic Speeds. NACA Rept. 1376, 1958. (Supersedes NACA TN 4045.)

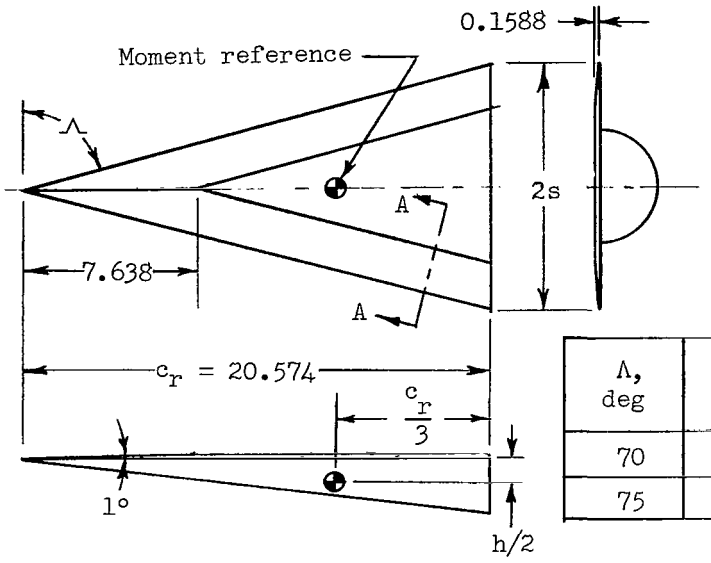

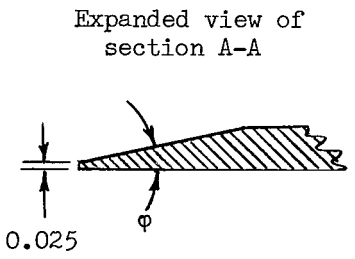

Λ, deg	s, cm	φ, deg	$\frac{V^{2/3}}{S}$ (body in place)
70	7.45	2.92	0.127
75	5.51	3.86	.177

(a) Wing dimensions with typical body in place.

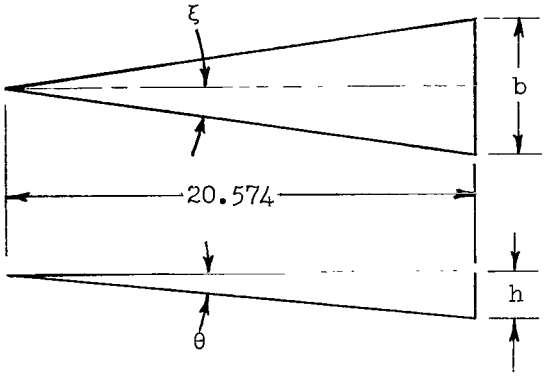

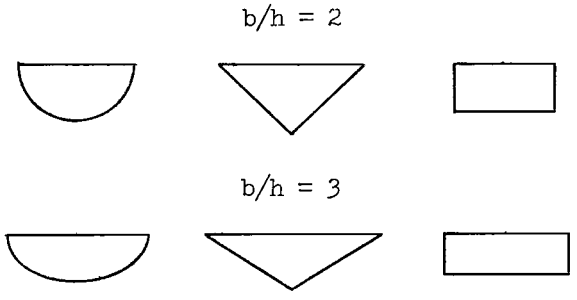

Cross section	b/h	ξ, deg	θ, deg	$V^{2/3}/S$	b/h	ξ, deg	θ, deg	$V^{2/3}/S$
Triangular	2	8.8	8.8	0.258	3	10.7	7.2	0.211
Rectangular	2	6.2	6.2	.365	3	7.5	5.0	.297
Elliptical	2	7.0	7.0	.324	3	8.6	5.7	.264

(b) Bodies.

Figure 1.- Configurations investigated. All dimensions except angle designations are in centimeters.

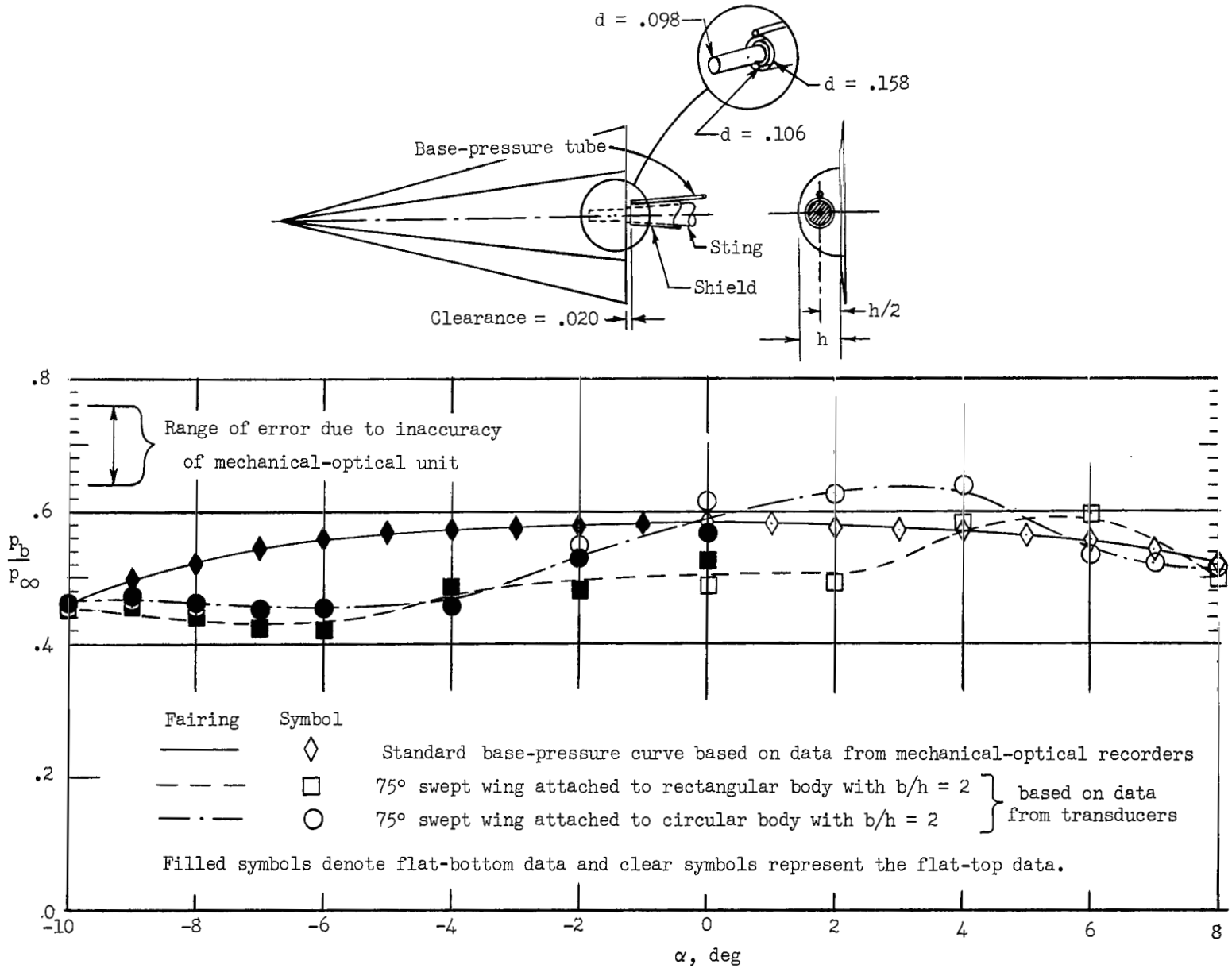

Figure 2.- Base-pressure values. Sketch dimensions are in centimeters.

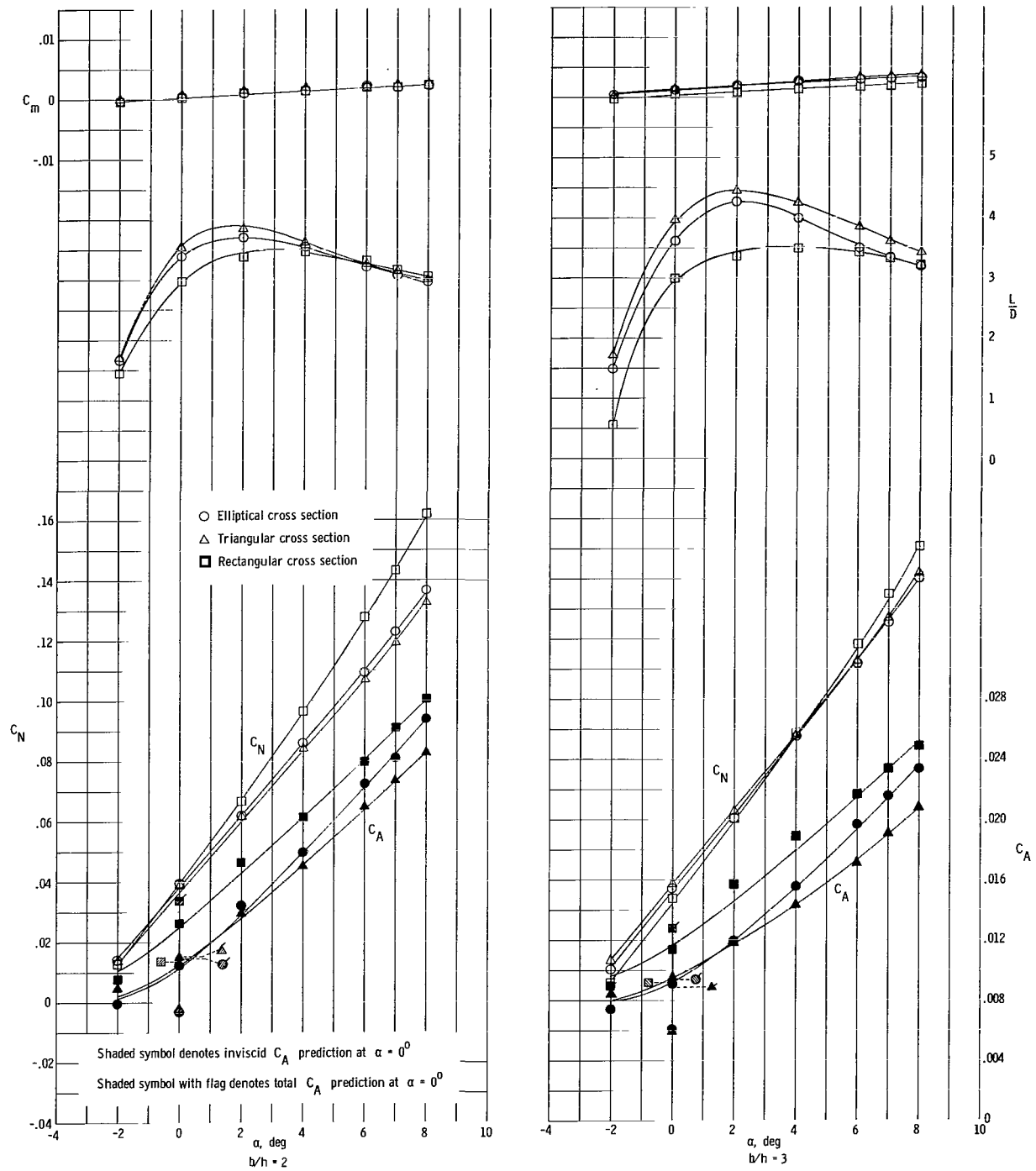

(a) Body alone (flat top).

Figure 3.- Basic data plots for various cross-section configurations. $R = 1.4 \times 10^6$.

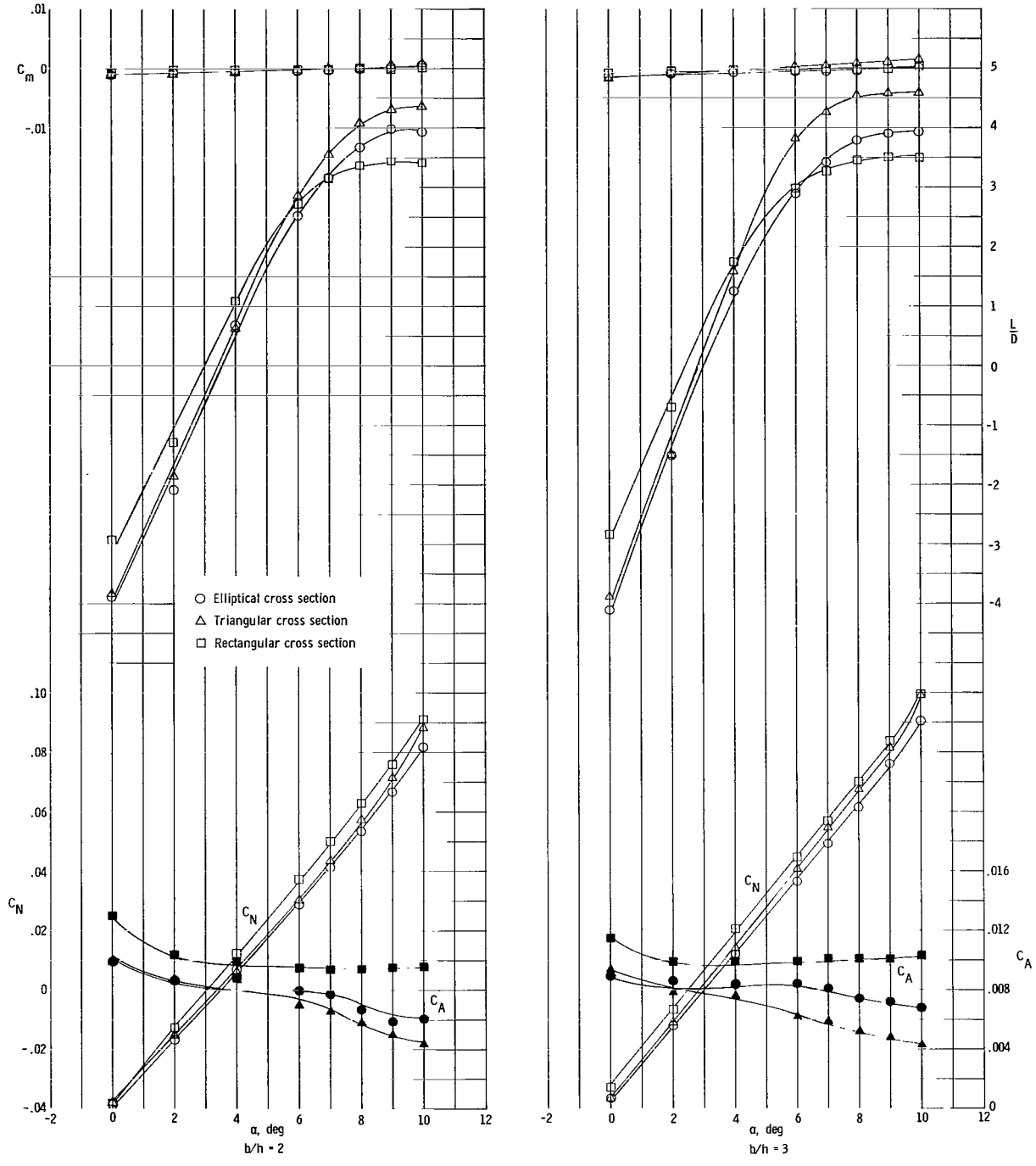

(b) Body alone (flat bottom).

Figure 3.- Continued.

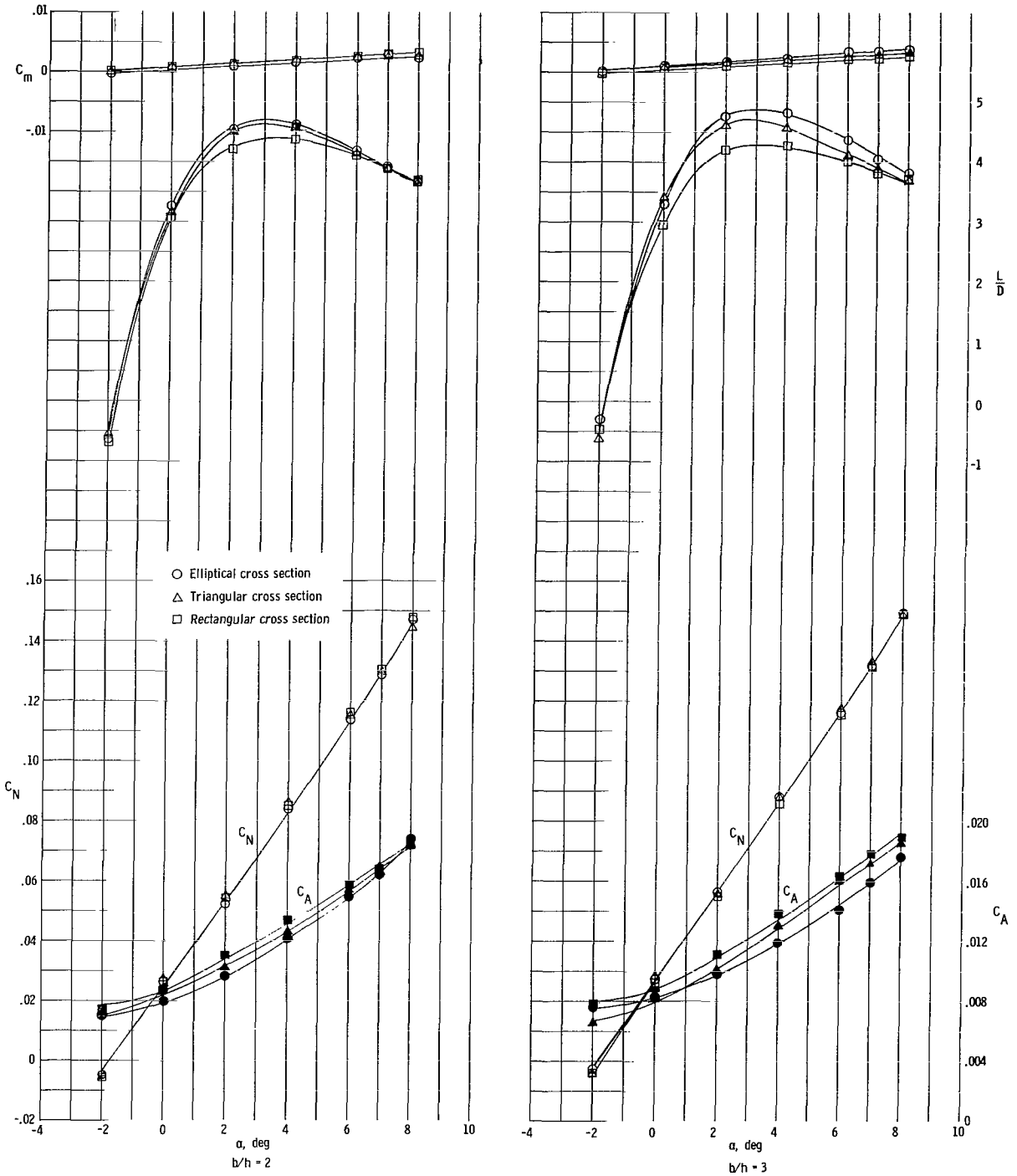

(c) 75° swept wing attached (flat top).

Figure 3.- Continued.

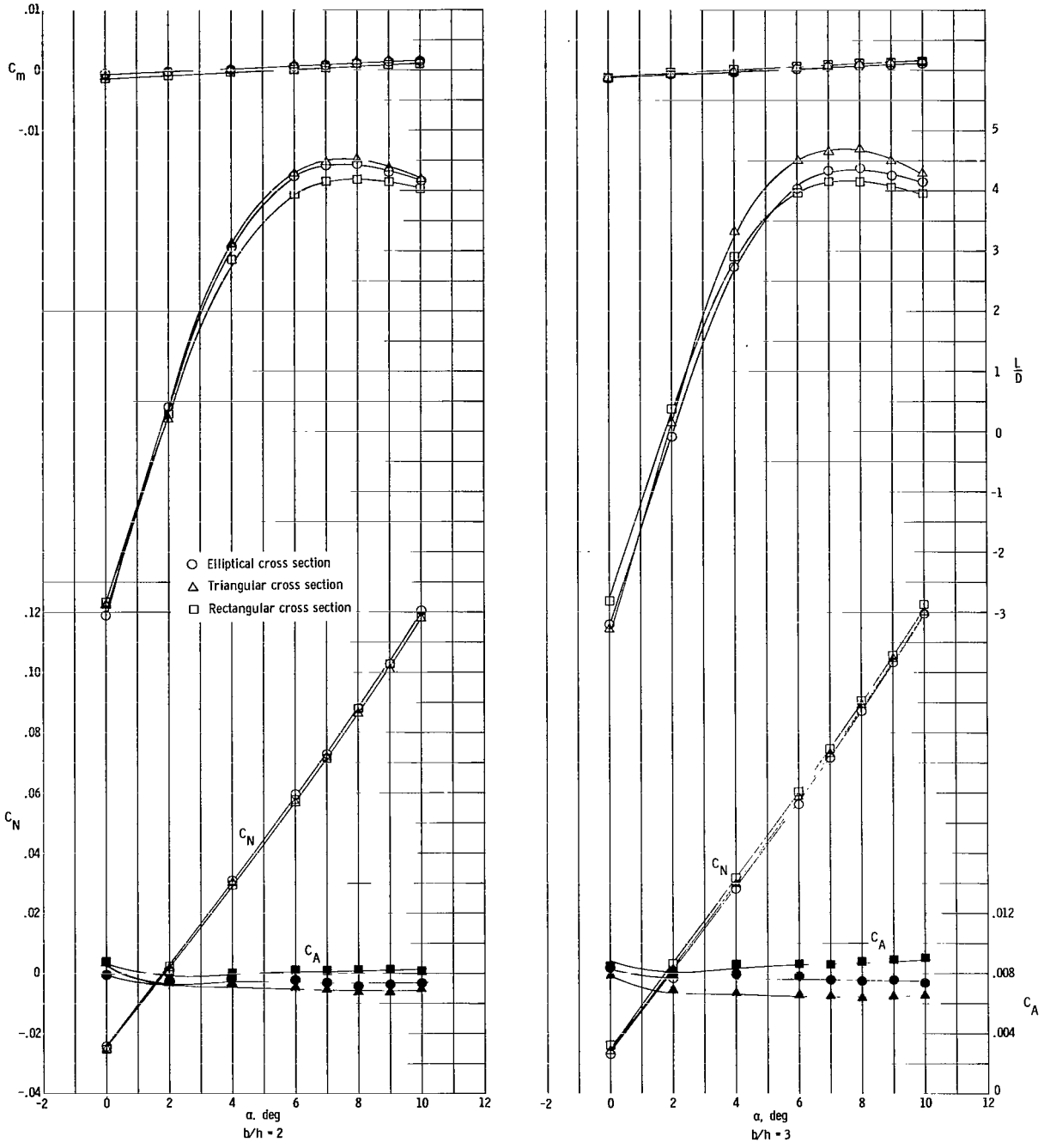

(d) 75° swept wing attached (flat bottom).

Figure 3.- Continued.

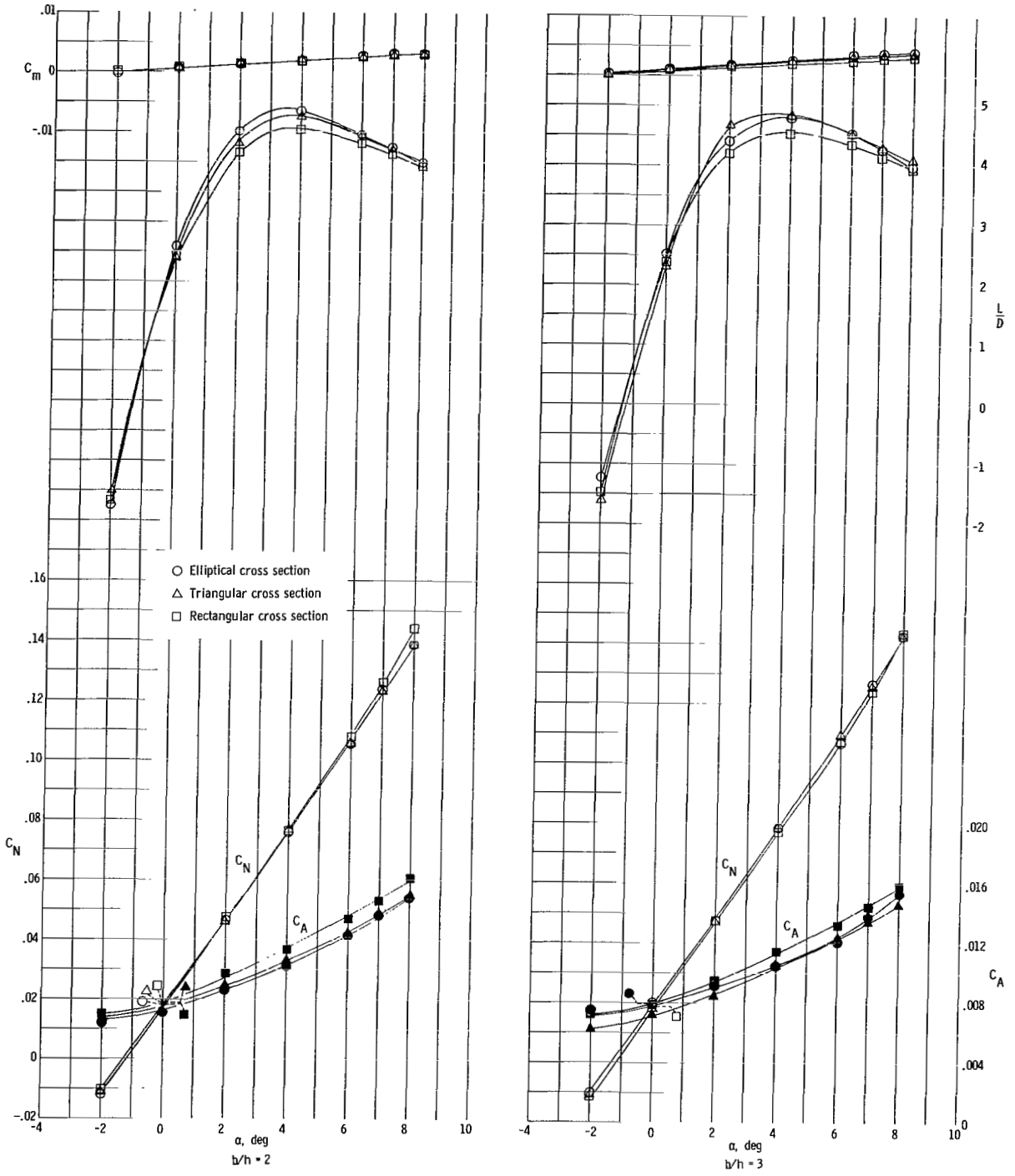

(e) 70^0 swept wing attached (flat top).

Figure 3.- Continued.

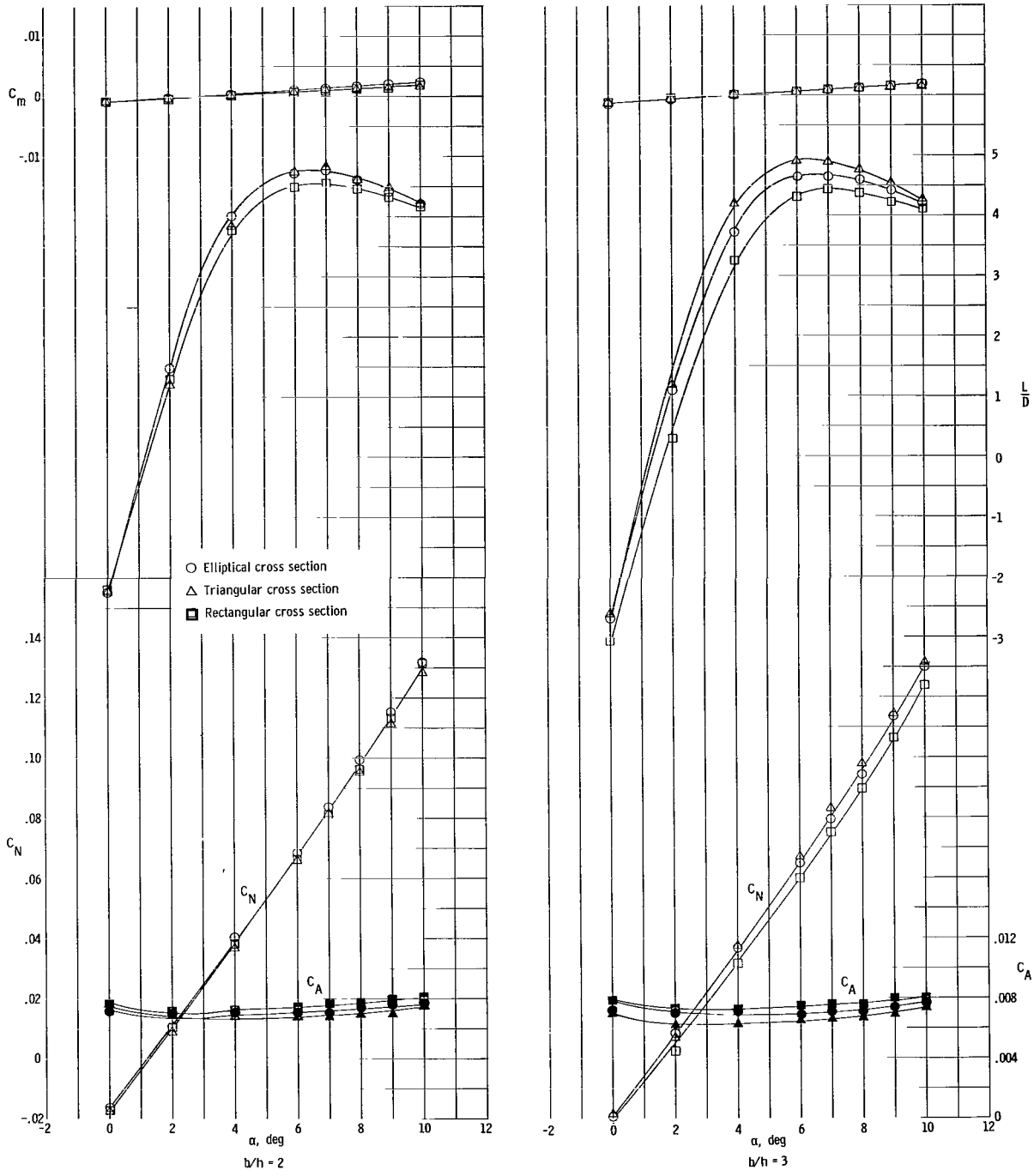

(f) 70^{o} swept wing attached (flat bottom).

Figure 3.- Concluded.

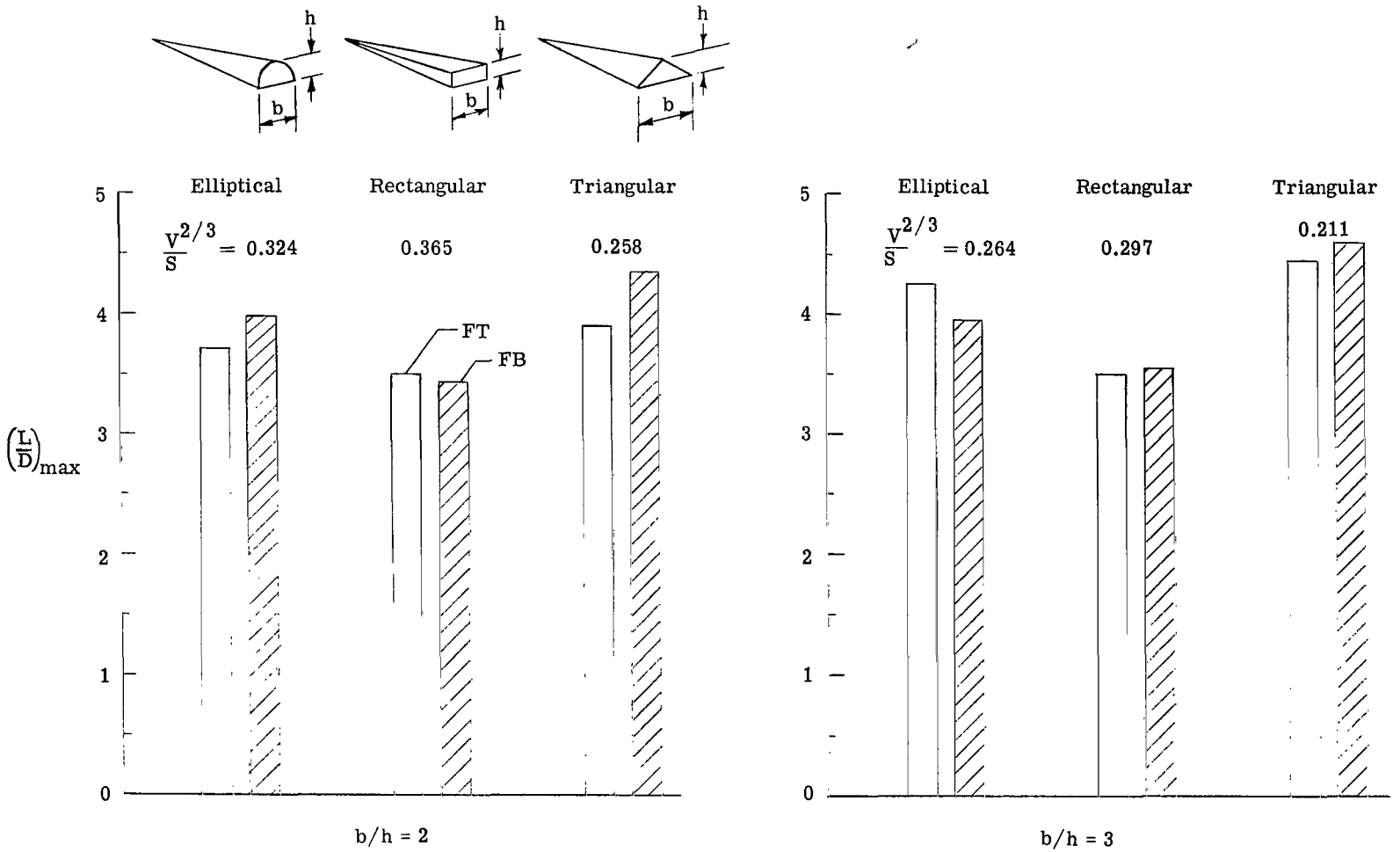

(a) Bodies alone. $R = 1.4 \times 10^6$.

Figure 4.- Aerodynamic efficiencies of various cross-section configurations.

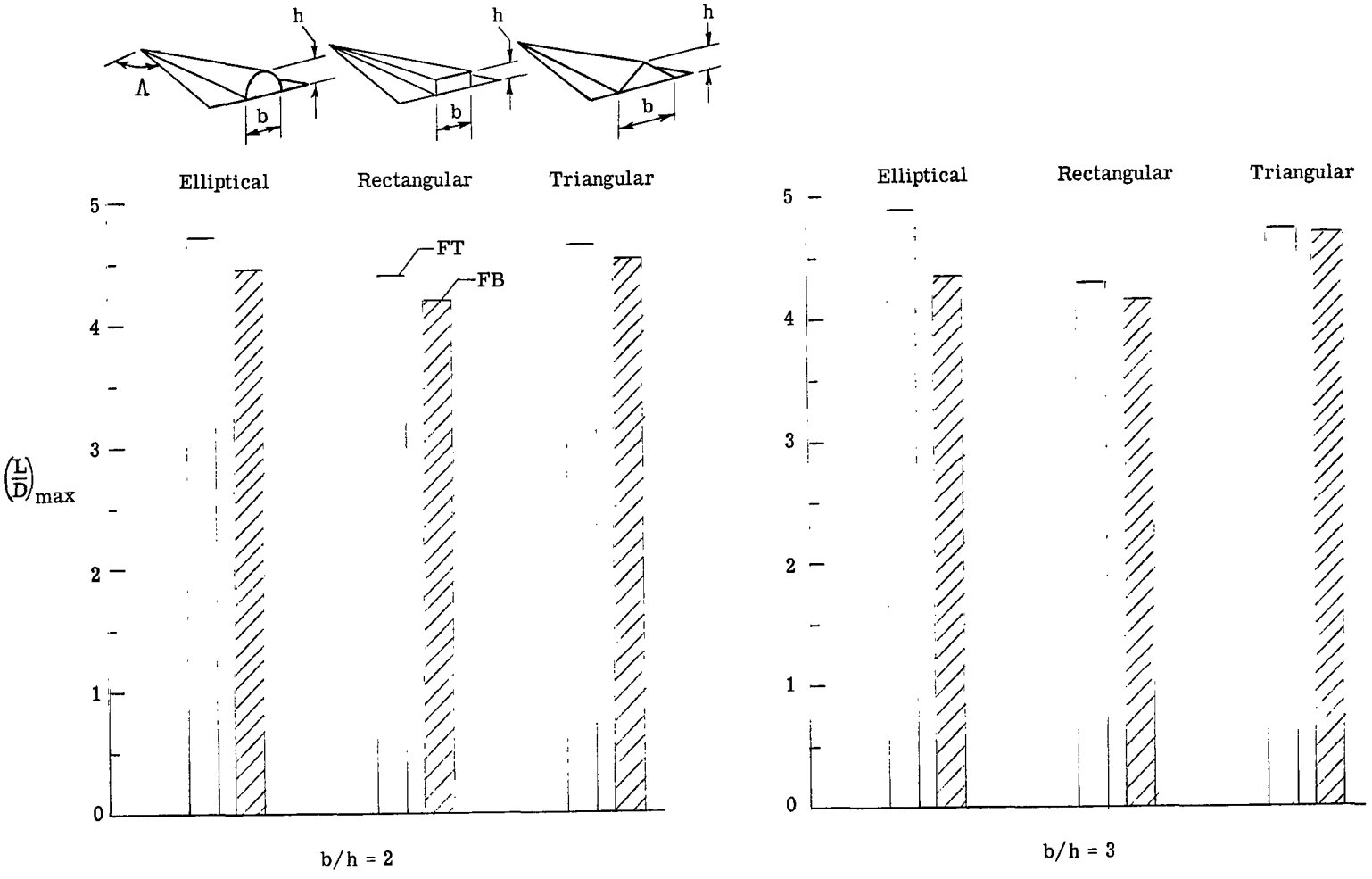

(b) 75° swept wing attached to bodies. $V^{2/3}/S = 0.177$; $R = 1.4 \times 10^6$.

Figure 4.- Continued.

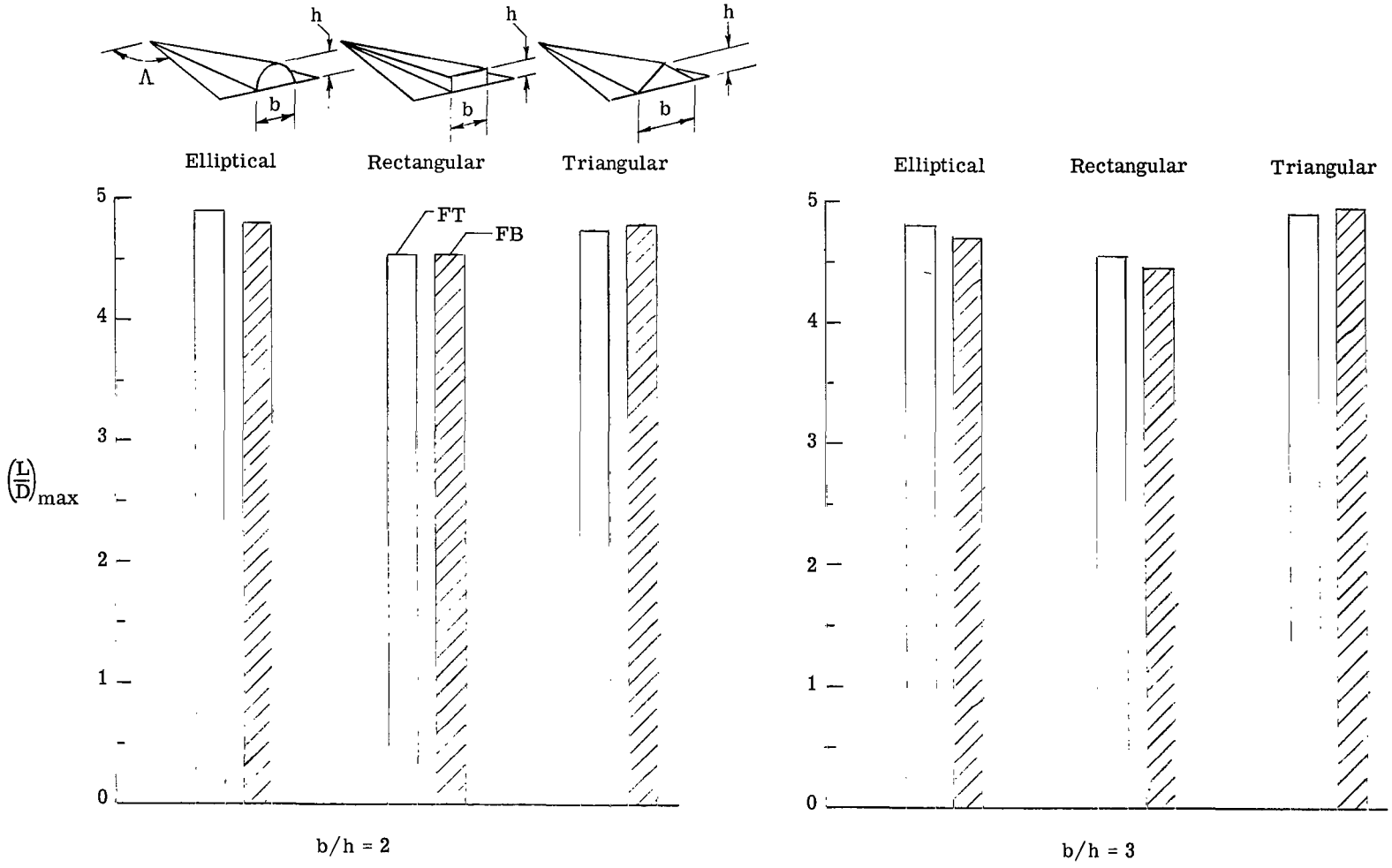

(c) 70° swept wing attached to bodies. $V^{2/3}/S = 0.126$; $R = 1.4 \times 10^6$.

Figure 4.- Concluded.

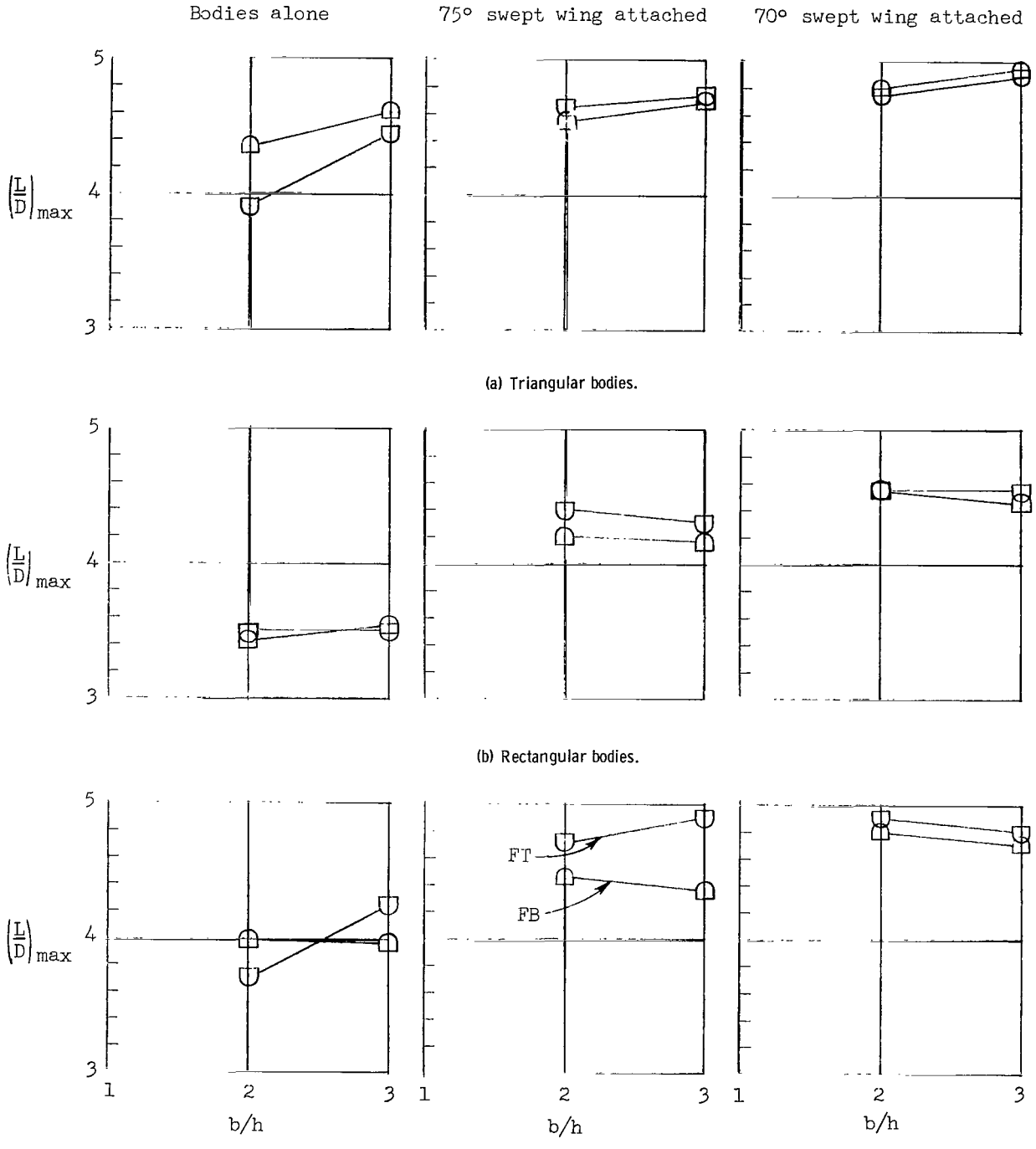

(a) Triangular bodies.

(b) Rectangular bodies.

(c) Elliptical bodies.

Figure 5.- Effect of width-height ratio on $(L/D)_{max}$. $R = 1.4 \times 10^6$.

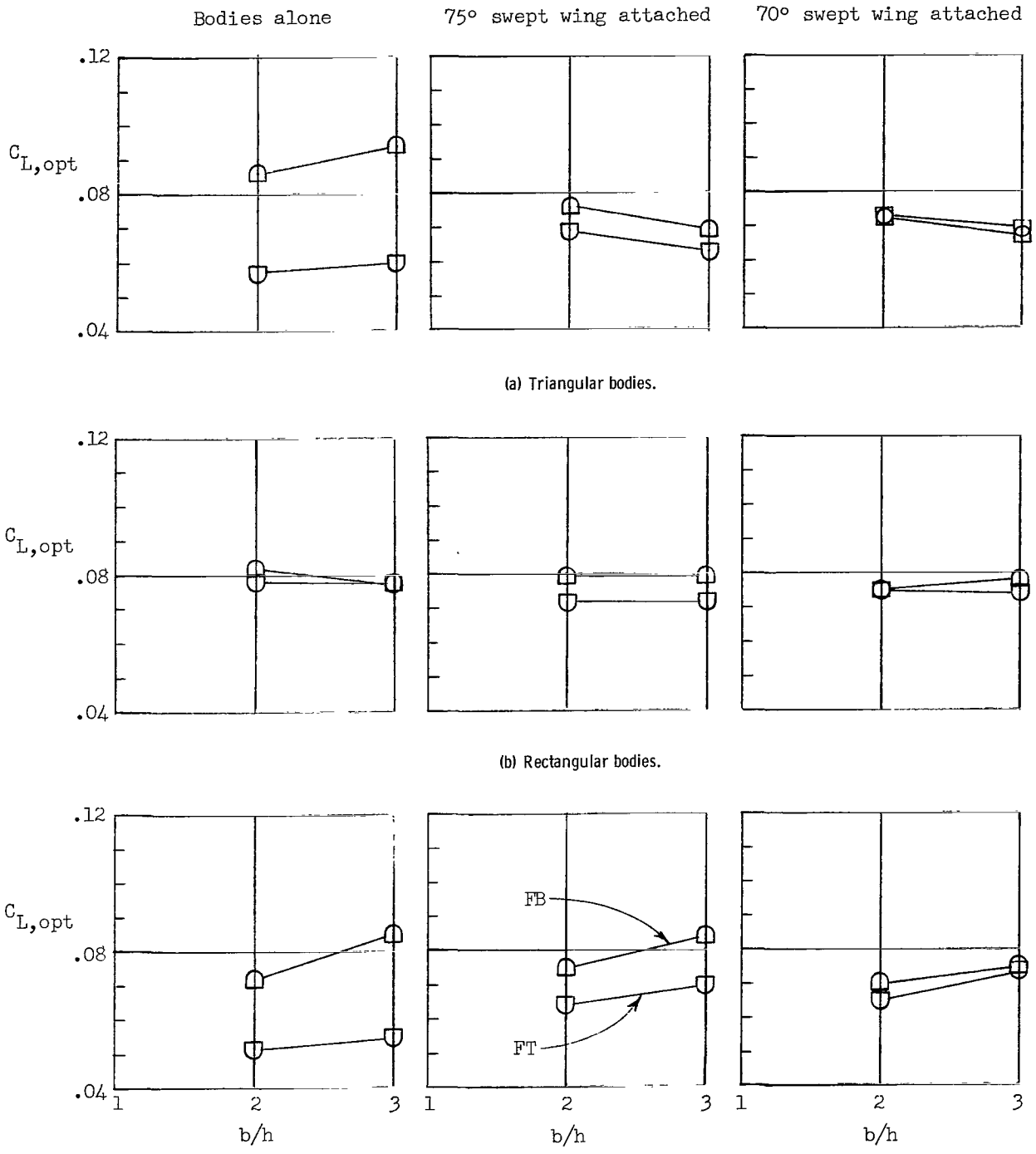

(a) Triangular bodies.

(b) Rectangular bodies.

(c) Elliptical bodies.

Figure 6.- Effect of width-height ratio on $C_{L,opt}$. $R = 1.4 \times 10^6$.

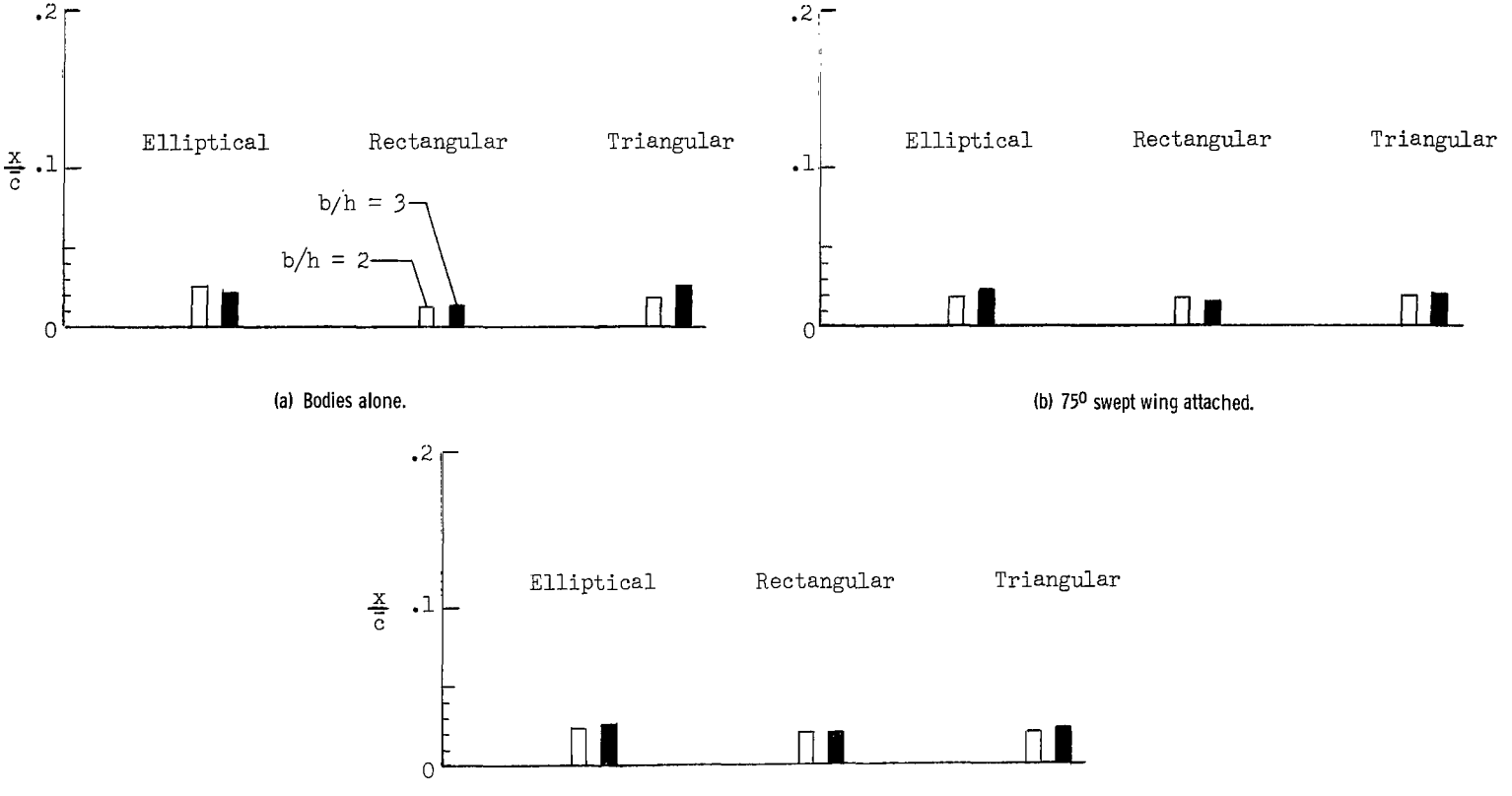

(a) Bodies alone.

(b) 75° swept wing attached.

(c) 70° swept wing attached.

Figure 7.- Effect of body cross-sectional shape on aerodynamic center. $R = 1.4 \times 10^6$.

"The aeronautical and space activities of the United States shall be conducted so as to contribute . . . to the expansion of human knowledge of phenomena in the atmosphere and space. The Administration shall provide for the widest practicable and appropriate dissemination of information concerning its activities and the results thereof."

—NATIONAL AERONAUTICS AND SPACE ACT OF 1958

NASA SCIENTIFIC AND TECHNICAL PUBLICATIONS

TECHNICAL REPORTS: Scientific and technical information considered important, complete, and a lasting contribution to existing knowledge.

TECHNICAL NOTES: Information less broad in scope but nevertheless of importance as a contribution to existing knowledge.

TECHNICAL MEMORANDUMS: Information receiving limited distribution because of preliminary data, security classification, or other reasons.

CONTRACTOR REPORTS: Technical information generated in connection with a NASA contract or grant and released under NASA auspices.

TECHNICAL TRANSLATIONS: Information published in a foreign language considered to merit NASA distribution in English.

TECHNICAL REPRINTS: Information derived from NASA activities and initially published in the form of journal articles.

SPECIAL PUBLICATIONS: Information derived from or of value to NASA activities but not necessarily reporting the results of individual NASA-programmed scientific efforts. Publications include conference proceedings, monographs, data compilations, handbooks, sourcebooks, and special bibliographies.

Details on the availability of these publications may be obtained from:

SCIENTIFIC AND TECHNICAL INFORMATION DIVISION

NATIONAL AERONAUTICS AND SPACE ADMINISTRATION

Washington, D.C. 20546